Synthesis and Properties of Organic/Inorganic Hybrid Nanoparticles Prepared Using Atom Transfer Radical Polymerization

Tzong-Liu Wang, Chia-Chih Ou, Chien-Hsin Yang

Department of Chemical and Materials Engineering, National University of Kaohsiung, Kaohsiung 811, Taiwan, Republic of China

Received 20 September 2007; accepted 18 March 2008
DOI 10.1002/app.28462
Published online 27 May 2008 in Wiley InterScience (www.interscience.wiley.com).

ABSTRACT: The synthesis of organic/inorganic hybrid materials was conducted by atom transfer radical polymerization (ATRP) of styrene and methyl methacrylate (MMA) from the surface of silica colloids. Colloidal initiators were prepared by the functionalization of silica nanoparticles with (3-(2-bromoisobutyryl)propyl) dimethylethoxysilane (BIDS). Well-defined polymer chains were grown from the nanoparticle surfaces to yield individual particles composed of a silica core and a well-defined outer polystyrene (PS) or poly(methyl methacrylate) (PMMA) layer. Fourier transform infrared (FTIR) and solid state ^{13}C and ^{29}Si-NMR spectroscopy confirmed the successful modification of nanosilica surfaces. Subsequent grafting of polymers on silica surfaces by ATRP was also performed with success based on FTIR and NMR data. Scanning electron microscopy (SEM) and silicon mapping showed both hybrid materials were homogeneous dispersion systems. Energy dispersive X-ray spectrometer (EDS) analysis indicated that the BIDS initiator was covalently attached on surfaces of silica nanoparticles and ATRP of styrene and MMA were accomplished. Thermogravimetric analysis (TGA) results displayed higher thermal stabilities for both nanohybrids in comparison with the linear-type vinyl polymers. Contact angle measurements revealed the nanomaterials character for both silica-based hybrid materials. © 2008 Wiley Periodicals, Inc. J Appl Polym Sci 109: 3421–3430, 2008

Key words: organic/inorganic hybrid materials; atom transfer radical polymerization; nanoparticles; colloidal initiators; contact angle

INTRODUCTION

The preparation of organic/inorganic hybrid materials composed of organic polymers and inorganic nanoparticles has attracted strong interest because of the combination of the advantageous properties of both classes of molecules into one material.[1–5] The organic polymer shell determines the chemical properties of such materials and their interaction with the environment, whereas their physical properties are governed by both the size and shape of the inorganic core and the surrounding organic layer. These materials exhibit novel size-dependent magnetic, optical, and materials properties that could find application in a wide array of technologies.[6–10] However, the exploitation of these properties requires a homogeneous dispersion of the particles in the polymer matrix. To avoid agglomeration in the hybrid materials, it is indicated that grafting polymer chains from a surface modified with polymerization initiators is the most effective method for this purpose.[11] In recent years, much attention has been paid to the use of atom transfer radical polymerization (ATRP) technique to graft polymer chains from surfaces of nanoparticles.[11–13] This approach would conduct a controlled/''living'' radical polymerization from the surface of an inorganic nanoparticle macroinitiator, yielding nanoparticles with an inorganic core and an outer layer of covalently attached, well-defined polymer chains. This process would afford control over the molecular weight, molecular weight distribution, and structure of the resulting polymer. For these reasons, this method has been investigated by several groups.[6,14–17] Recently, the functionalization of various colloids, including silica,[6,16–21] gold,[22–24] silver,[25] germanium,[26] carbon black,[27] PbS,[28] metal oxide systems,[29–31] and other surfaces,[32,33] was achieved. The functionalized colloids were applied as initiators for the ATRP of vinyl monomers. The use of ATRP in the synthesis of these nanoparticle hybrids will allow for control of polymer structure and will be conducive to the construction of a wide variety of macromolecular architectures. A well-controlled synthesis

Correspondence to: T. L. Wang (tlwang@nuk.edu.tw).
Contract grant sponsor: National Science Council of Republic of China; contract grant number: 93-2216-E-390-004.
Contract grant sponsor: Ministry of Education; contract grant number: 0960190683Q.

for these materials can lead to the creation of an entire new category of materials with structures that are controllable on the nanometer scale.

However, to our knowledge, little experimental study has been performed on the structure characterization and properties of such hybrid materials. Most researches lay emphasis only on the discussions of kinetics and reaction conditions of ATRP process.[17,34–37] Herein, we report not only the synthesis, but also characterization and properties study of hybrid nanoparticles composed of a silica colloidal core and of an outer shell of tethered polymers. In this research, ATRP of styrene and methyl methacrylate monomers were carried out on the functionalized nanosilica surfaces. Solid state ^{13}C and ^{29}Si nuclear magnetic resonance (NMR) spectra were used in the characterization of the colloidal initiators and the hybrid materials. In addition, scanning electron microscopy (SEM), energy dispersive X-ray spectrometer (EDS), thermogravimetric analysis (TGA), and contact angle measurements, etc., were also performed to investigate the morphology and properties of these hybrid materials.

EXPERIMENTAL

Materials

The silica nanoparticles (MW = 60.09 g/mol) bearing surface silanol groups (10.3 mmol/g) were purchased from Desunnano Co., Ltd.; the purity is higher than 99% and the polydispersity is 1.20. The surface area and particle size are 640 m^2/g and 10 nm, respectively. Toluene (Janssen Chimica), styrene (St, Tokyo Chemicals), methyl methacrylate (MMA, Tokyo Chemicals), allyl-2-bromoisobutyrate (Aldrich) were distilled under reduced pressure. Tetrahydrofuran (THF, Nihon Shiyaku) was distilled before use. CuBr (Acros, 98%) was purified by washing with glacial acetic acid, followed by absolute ethanol and ethyl ether, and then dried under vacuum. 2, 2′-Bipyridyl (bipy, Hayashi Chemicals, 99.9%), hydrogen hexachloroplatinate hexahydrate (Showa Chemicals), ethoxydimethylsilane (Lancaster) were used as received. All other reagents were used as received.

Synthesis of (3-(2-bromoisobutyryl)propyl) dimethylethoxysilane (BIDS)

To a round bottom flask containing 3.4 mL (0.021 mmol) of allyl-2-bromoisobutyate was added 0.05 mL (0.12*M*, 0.006 mmol) of hydrogen hexachloroplatinate hexahydrate catalyst. Ethoxydimethylsilane 4 mL (0.029 mmol) was added dropwise and the reaction was heated at 45°C for 48 h. The disappearance of the vinyl protons was monitored via ^1H-NMR. The hydrosilated product was recovered in a 69% yield (5.11 g) by distillation at 75°C (20 mTorr). The reaction is given in Scheme 1.

FTIR (KBr, cm^{-1}): 2962 (ν_{C-H}), 1745 ($\nu_{C=O}$), and 1096 ($\nu_{Si-O-Si}$). ^1H-NMR (δ, ppm, $CDCl_3$): 0.08 (s, 6H, CH_3—Si—CH_3), 0.55 (m, 2H, CH_2—CH_2—Si), 1.13 (t, 3H, O—CH_2CH_3), 1.68 (m, 2H, CH_2—CH_2—Si), 1.92 (s, 6H, CH_3—C—CH_3), 3.70 (q, 2H, O—CH_2CH_3), 4.08 (m, 2H, O—CH_2—CH_2—CH_2).

Preparation of silica colloidal initiator (SiO_2-BIDS)

Silica surface ATRP initiator was prepared by reflux reaction of 0.75 g (bearing surface silanol groups 7.73 mmol) silica nanoparticles and excess BIDS (∼ 1.5 mol equivalents) 3.60 g (11.6 mmol) in 7.5 mL of THF for 15 h using a three-necked round bottom flask fitted with a Dean-Stark trap. The obtained particles were isolated by precipitation in hexane and followed by centrifugation to remove the unreacted BIDS. The particles were washed free of any adsorbed BIDS with hexane followed by centrifugation and resuspension in hexane. The centrifugation/resuspension was repeated for five times, and then volatile materials were removed under vacuum. Purity of the obtained product was verified by thin layer chromatography (TLC) and NMR analysis. For TLC analysis, wherein a mixed solvent of hexane and ethyl acetate (hexane:ethyl acetate = 2 : 3, V/V) was used as a mobile phase to develop the solution drop in a silica gel TLC film. By comparing the TLC migration behavior of the obtained particles with the pure sample of BIDS, the identity and purity of the colloidal initiator can be determined. This initiator was designated as SiO_2-BIDS. The reaction is also shown in Scheme 1.

ATRP of Styrene or MMA from BIDS functionalized colloids

Styrene (4.37 g, 0.042 mol), CuBr (60.2 mg, 0.42 mmol), and bipy (130 mg, 0.83 mmol) were introduced into a glass flask, which was then capped by a three-way stopcock and purged with nitrogen by repeated vacuum/nitrogen cycles. The silica colloidal initiator (48.2 mg, bearing ∼ 0.21 mmol initiating groups) in toluene (3.86 g, 0.042 mol) was then added under nitrogen with a syringe. The reaction mixture was then heated at 100°C for 8 h. Afterwards, the flask was removed from the oil bath and the reaction mixture diluted with THF. The solution was filtered through a column with neutral alumina to remove the catalyst. The polymer/silica hybrid was recovered by precipitation in methanol, followed by drying at 70°C for 24 h under high vacuum. ATRP of MMA was carried out in a similar manner.

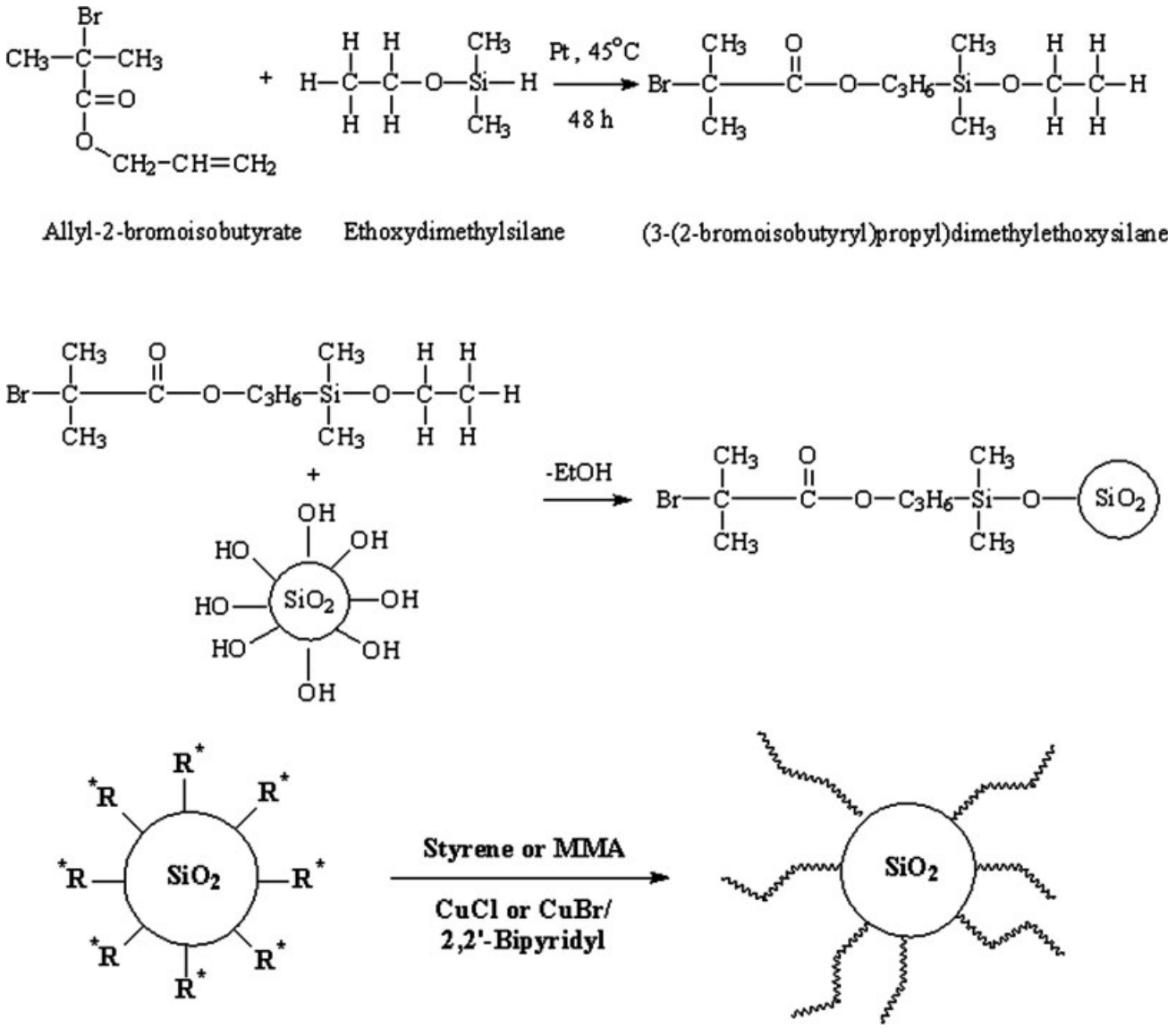

Scheme 1 Synthetic route for the preparation of organic/inorganic hybrid nanoparticles.

Characterization

Infrared spectra of samples were obtained using a Bio-Rad FTS 165 Fourier transform infrared (FTIR) spectrometer. The spectra were obtained over the frequency range of 4000–400 cm^{-1} at a resolution of 4 cm^{-1}.

The silica cores of the hybrid materials were etched with aqueous HF solution for obtaining the neat polymers.

The synthesized compounds and polymers were dissolved in deuterated chloroform ($CDCl_3$), and then characterized with ^{1}H-NMR using a Varian UNITY INOVA-500 FT-NMR spectrometer.

Solid state ^{13}C and ^{29}Si-NMR spectra were recorded by means of polarization transfer from ^{1}H nuclei and magic angle spinning (CP-MAS) on a Bruker Avance 400 spectrometer. The spinning rate was 5 kHz.

Number average ($\overline{M}_n$), weight average ($\overline{M}_w$) molecular weights and molecular weight distributions (MWDs) ($\overline{M}_w/\overline{M}_n$) were determined by gel permeation chromatography (GPC) using Waters liquid chromatograph equipped with a 410 RI detector and three μ-Styragel columns with THF as the carrier solvent.

TGA experiments were carried out on the samples placed in a platinum sample pan using a TA Instruments SDT-2960 analyzer. Samples ranging from 4 to 5 mg were loaded into the platinum pan and sealed in the sample chamber. The samples were heated from 50 to 700°C under a nitrogen atmosphere at the rate of 20°C/min.

TABLE I
GPC Results of the Surface-Grafted Polymers and Final Conversions of the ATRP Reactions

Polymer	$\overline{M_n}$ (g/mol)	$\overline{M_w}$ (g/mol)	PDI	Conversion (%)
PS	17300	21500	1.24	26.5
PMMA	24300	30800	1.27	41.8

A GBX Digidrop contact angle goniometer was employed to measure the contact angle of water on polymer/silica hybrids coated glass slides, using the sessile drop technique.

The morphology of the fractured surfaces of the hybrid materials and EDS analysis were examined with SEM (JEOL 5610, Japan).

The distributions of Si atoms in the macroinitiator and hybrid materials were obtained from SEM EDS mapping (JEOL 5610, Japan). The white points in the figures denote Si atoms.

RESULTS AND DISCUSSION

Preparation of silica colloidal initiator and ATRP of St and MMA

In this research, we aimed at the synthesis of structurally well-defined polymer-nanoparticle hybrids obtained by ATRP of styrene or MMA with surface-modified silica initiator. In this method, ATRP is used to conduct a controlled/living polymerization from the surface of a silica nanoparticle macroinitiator, yielding a nanoparticle with an inorganic core and an outer layer of covalently attached, well-defined polymer chains (Scheme 1).

To execute ATRP of St or MMA, a silica nanoparticle macroinitiator must be used. Before preparation of the silica colloidal macroinitiator, a hydrosilated alkyl halide initiator must be synthesized. The hydrosilated alkyl halide BIDS was synthesized by the reaction of allyl-2-bromoisobutyate and ethoxydimethylsilane. The chemical structure of BIDS was identified by FTIR and ^{1}H-NMR and shown in Experimental section. The preparation of the silica nanoparticle macroinitiator was carried out by the condensation reaction of BIDS with the surface silanol groups of silica nanoparticles. To ensure the completion of the reaction, a Dean-Stark trap was used to help the removal of the condensate ethanol. Since the halogen-containing silica nanoparticle macroinitiator was insoluble in common organic solvents, the identification and characterization were conducted by FTIR and solid state NMR.

The surface-modified nanosilica initiator (SiO_2-BIDS) was used as the macroinitiator for ATRP of styrene and methyl methacrylate. The molecular weights and molecular weight distributions of the grafted polymer were obtained by etching the silica cores with aqueous HF solution. The molecular weight of the polymer arms, as determined using GPC, increased with the polymerization conversion, and the molecular weight distribution remained narrow after the initial stages of the polymerization. Data of molecular weight and molecular weight distribution (i.e., polydispersity index (PDI)) of the resultant polystyrene (PS) and poly(methyl methacrylate) (PMMA) are shown in Table I. In addition, Figures 1 and 2 show plots of $\overline{M_n}$ versus conversion, and monomer conversion versus time for the ATRP of styrene and MMA from BIDS colloidal initiators Both figures exhibited the characteristics of a controlled/''living'' polymerization. It is apparent seen from Table I that both samples have PDI values

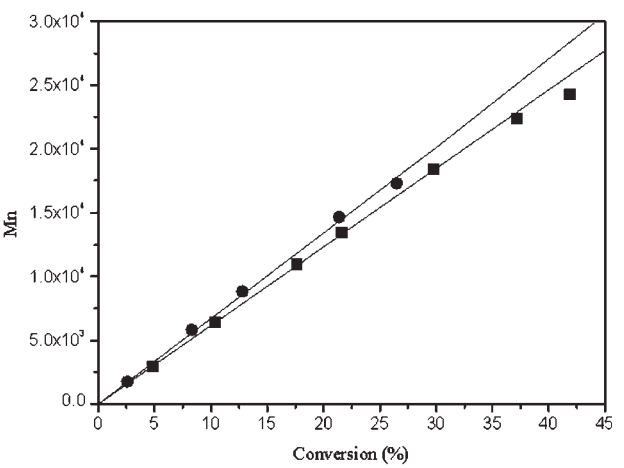

Figure 1 Plot of $\overline{M_n}$ versus conversion for the ATRP of styrene (filled circles) and MMA (filled squares) from BIDS colloidal initiators using stoichiometric ratios of 100 : 0.5 : 1 : 2 for $[M]_0$: $[I]_0$: $[CuBr]_0$: $[bipy]_0$ in toluene at 100°C.

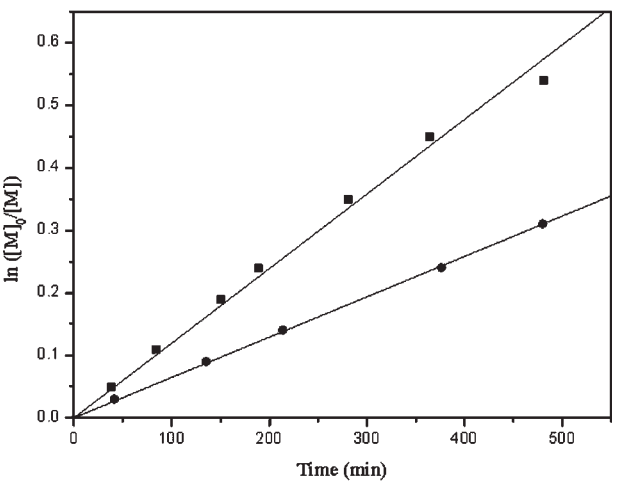

Figure 2 Semilogarithmic plots of monomer conversion versus time for the ATRP of styrene (filled circles) and MMA (filled squares), using BIDS colloidal initiators at stoichiometric ratios of 100 : 0.5 : 1 : 2 for $[M]_0$: $[I]_0$: $[CuBr]_0$: $[bipy]_0$ in toluene at 100°C.

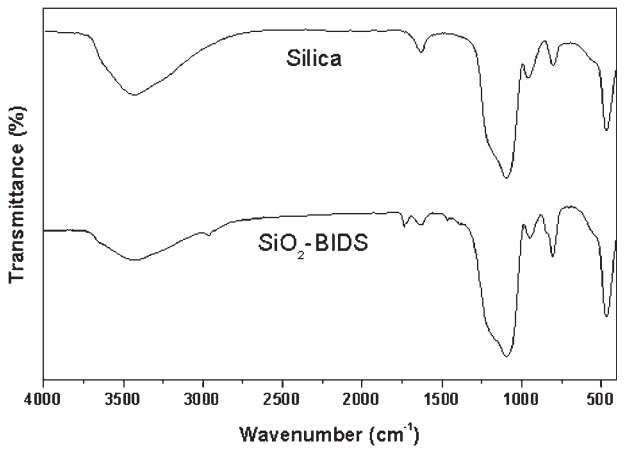

Figure 3 FTIR spectra of silica and SiO_2-BIDS.

lower than 1.5, and the characteristics of Figures 1 and 2, indicating ATRP of styrene and MMA by the SiO_2-BIDS macroinitiator was successful.

Infrared and solid state ^{29}Si-NMR characterization of SiO_2 and SiO_2-BIDS

Typical IR spectra of SiO_2 and SiO_2-BIDS are illustrated in Figure 3. IR spectra of both samples are similar as seen in the figure. For both samples, the absorption bands show the characteristic absorptions of typical SiO_2. The peaks appear at 1092 cm^{-1} are attributed to the absorption bands of Si—O—Si. The band at 949 cm^{-1} is assigned to the Si—OH stretching of silanol groups on the silica particles, while the peak at 3430 cm^{-1} is ascribed as the absorption of hydroxyl groups on the surface of nanosilica particles. In addition, a band due to SiO—H bending vibration is present at 1630 cm^{-1}. For SiO_2-BIDS, a C—H stretch is visible at 2963 cm^{-1} and a C=O stretch is observed at 1700 cm^{-1}, and both of these signals are not present in the spectrum of the unmodified (pristine) nanoparticles. Furthermore, the Si—O—Si stretch at 1092 cm^{-1} due to bulk silica remained a prominent feature in the spectrum. These results indicate that the chemical structure of SiO_2-BIDS is in accordance with our design.

Figure 4 shows the solid-state ^{29}Si CP-MAS NMR spectroscopy of the neat silica particles and BIDS-modified silica nanoparticles. In the spectrum of neat silica nanoparticles, the chemical shifts of the Q^2, Q^3, and Q^4 silicon nuclei of bulk silica are observed as a trimodal signal at −91.2, −100.1, and −108.5 ppm, respectively. Here, Q^n indicates the SiO unit with formula of $Si(OSi)_n(OH)_{4-n}$. The major constituents were Q^3 and Q^4 species for the silica nanoparticles, and Q^2 was barely detected. From the spectrum of BIDS-modified silica nanoparticles, it is obvious that the sum of area of Q^2 and Q^3 decreases and area of Q^4 increases as compared to those of pristine silica nanoparticles. Since the resonances of Q^2 and Q^3 represent the silanol groups on the silica surface, the decrease of total peak area for Q^2 and Q^3 indicates that surface silanols of silica particles have reacted with BIDS to form the ATRP initiator on silica surface. From the proportion of total integration area of Q^2 plus Q^3, and of Q^4 (i.e., total area of (Q^2 + Q^3)/area of Q^4), the conversion of surface silanol groups with BIDS was calculated to be ~ 43.1%. Since the silica nanoparticles bear 10.3 mmol/g surface silanol groups, the functionality of SiO_2-BIDS as macroinitiator for ATRP was calculated to be ~ 4.44 mmol/g.

Infrared and solid state ^{13}C, ^{29}Si-NMR characterization of PS/silica and PMMA/silica hybrids

Figure 5 shows the IR spectra of PS/silica and PMMA/silica hybrids. For the PS/Silica hybrid, the absorption bands of Si—O—Si appear at 465 and 1094 cm^{-1}. The band around 3059 cm^{-1} is assigned to the C—H stretch of aromatic ring. Two peaks at 1455 and 1494 cm^{-1} are attributed to C=C aromatic ring breathing. Other key features such as the absorption bands at 750 and 699 cm^{-1} also show

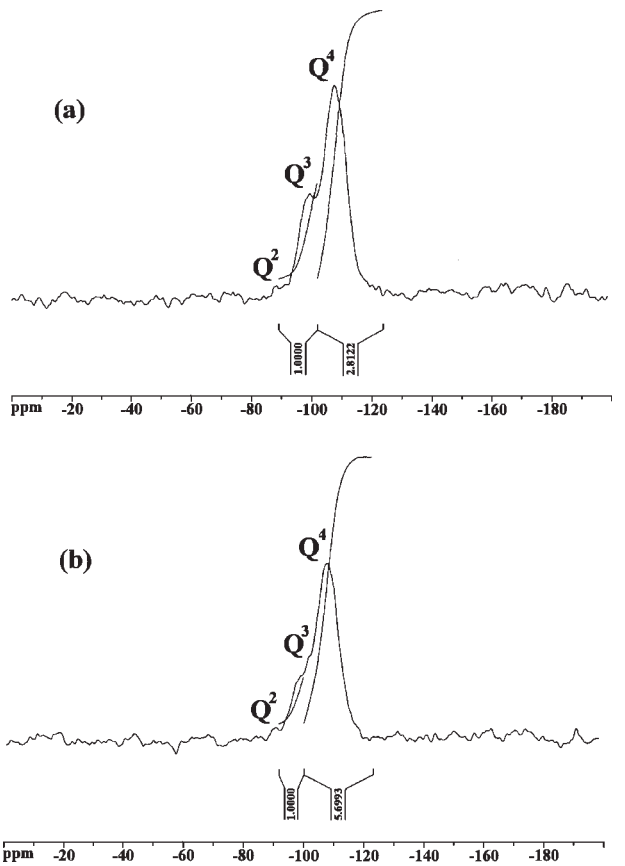

Figure 4 Solid-state ^{29}Si-NMR Spectra of (a) silica nanoparticles and (b) SiO_2-BIDS.

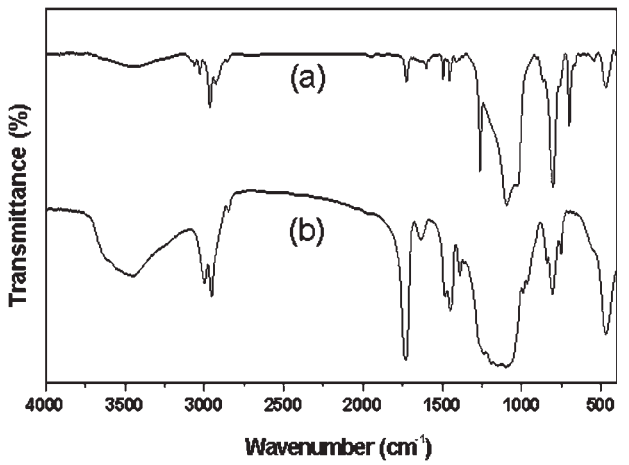

Figure 5 IR spectra of (a) PS/silica hybrid and (b) PMMA/silica hybrid.

characteristic absorptions of typical aromatic rings with five adjacent free hydrogen atoms. This spectrum proves clearly that the PS/silica hybrid has been successfully synthesized.

Subsequently, as compared to the IR spectrum of pristine silica (Fig. 3), the IR spectrum of PMMA/silica hybrid clearly shows the presence of PMMA segment. Two peaks at 2953 and 2848 cm^{-1} are ascribed as $—CH_3$ and $—CH_2—$ stretch, respectively. The carbonyl absorption appears at 1730 cm^{-1}. Peaks at 1486, 1451, and 1389 cm^{-1} are attributed to $—CH_3$ assymmetric, $—CH_2—$ symmetric, and $—CH_3$ symmetric bending, respectively. These results indicate that the PMMA segment has been incorporated into the organic/inorganic hybrid. The existence of PMMA polymer in the hybrid sample prepared from ATRP was well supported by the FTIR results.

Figure 6(a) shows the solid-state ^{13}C CP-MAS NMR of PS/silica hybrid. Peaks at 41.1 and 46.3 ppm observed in this spectrum are assigned to resonances of $CH—CH_2$. The peak at 147.5 ppm and 129.3 ppm are attributed to resonances of carbon of the phenyl ring attached to the backbone and the rest carbons of phenyl ring, respectively. On the other hand, the solid-state ^{13}C-NMR of PMMA/silica hybrid is shown in Figure 6(b). The peak detected at 177.6 ppm represents the resonance of $O—C=O$. Other signals at 55.0, 52.0, 45.3, and 16.8 ppm are ascribed as resonances of $—CH_2—C—$, $—OCH_3$, $—CH_2—C—$, and $—CH_3$, respectively. The aforementioned results also reveal the successful preparation of PS/silica and PMMA/silica hybrids.

Further confirmation of PS or PMMA covalently attached to silica nanoparticles was shown by solid-state ^{29}Si-NMR. As seen in Figure 7(a), the peak at 7.1 ppm is related to $—CH_2Si(CH_3)_2O—$, which is assigned to the resonance of the silicon nucleus of the surface-bound initiator. In addition, peaks of Q^2, Q^3, and Q^4 are also present. It is obvious that total area of Q^2 plus Q^3 decreases while area of Q^4 increases as compared to those of pristine nanosilica, indicating reaction of surface silanols with BIDS has occurred and ATRP of styrene has been successfully carried out. A similar phenomenon is observed for the PMMA/silica hybrid [Fig. 7(b)]. The peak at 9.1 ppm is also related to $—CH_2Si(CH_3)_2O—$ with a little shift in comparison with that of PS/silica hybrid.

SEM

To investigate the distribution of organic and inorganic phase in matrices of PS/silica and PMMA/silica hybrids, the morphology of the fractured surfaces of both samples was observed by SEM (Fig. 8). In both photographs, brittle hybrid structures con-

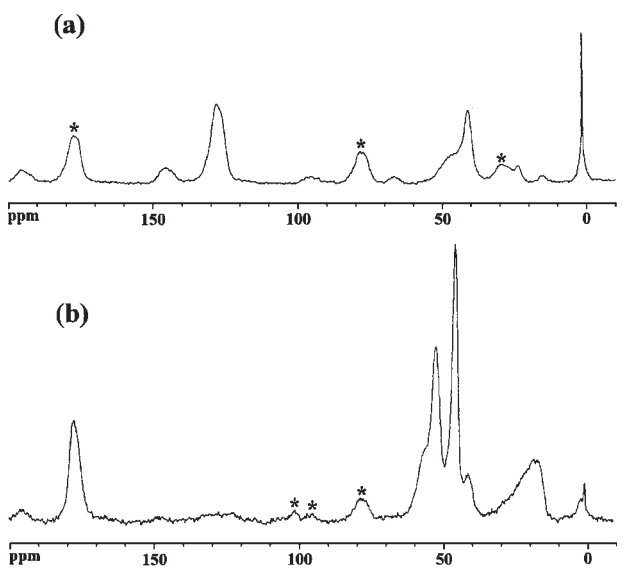

Figure 6 Solid-state ^{13}C-NMR of (a) PS/silica hybrid and (b) PMMA/silica hybrid Asterisks (*) denote spinning side bands.

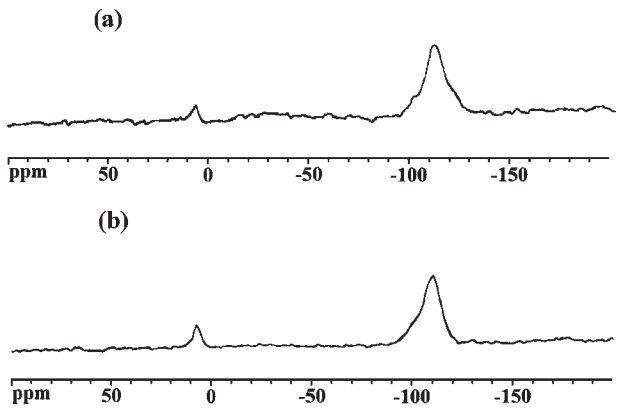

Figure 7 Solid-state ^{29}Si-NMR of (a) PS/silica hybrid and (b) PMMA/silica hybrid.

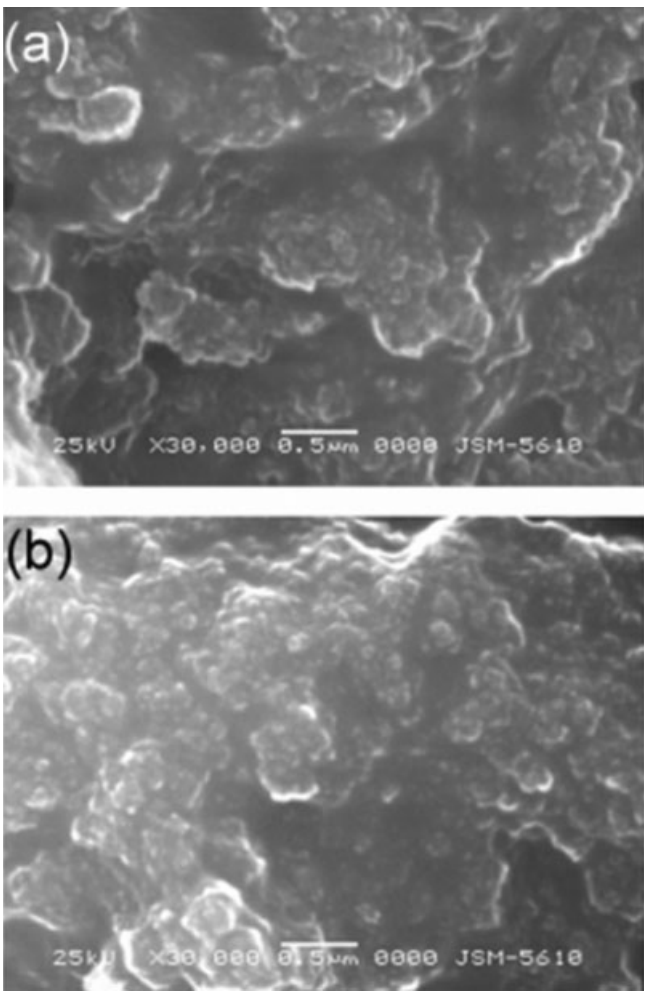

Figure 8 SEM micrographs of (a) PS/silica hybrid and (b) PMMA/silica hybrid.

sisting of a continuous matrix of polymer with the silica nanoparticles evenly dispersed throughout were observed. Comparing to the micron bar of micrographs, the particle sizes of silica particles (revealed as the lighter discrete particles) are in the nanoscale. These results show that silica networks are restrained under molecular level in the PS/silica and PMMA/silica hybrids.

SEM EDS and mapping

The distribution of silica in the SiO_2-BIDS macroinitiator and both hybrids was also observed by a SEM mapping technique. In the silicon mapping photographs (Fig. 9), the silica particles are uniformly dispersed in the macroinitiator and polymer matrix. EDS analysis was also conducted to detect the elemental compositions in SiO_2-BIDS and both nanohybrids. AS shown in Figure 10, EDS analysis on the macroinitiator and both hybrid samples produced strong carbon, oxygen, and silicon signals. EDS results also show that bromine was present in these samples, indicating the BIDS initiator was covalently attached on surfaces of silica nanoparticles and ATRP of styrene and MMA was successful. In addi-

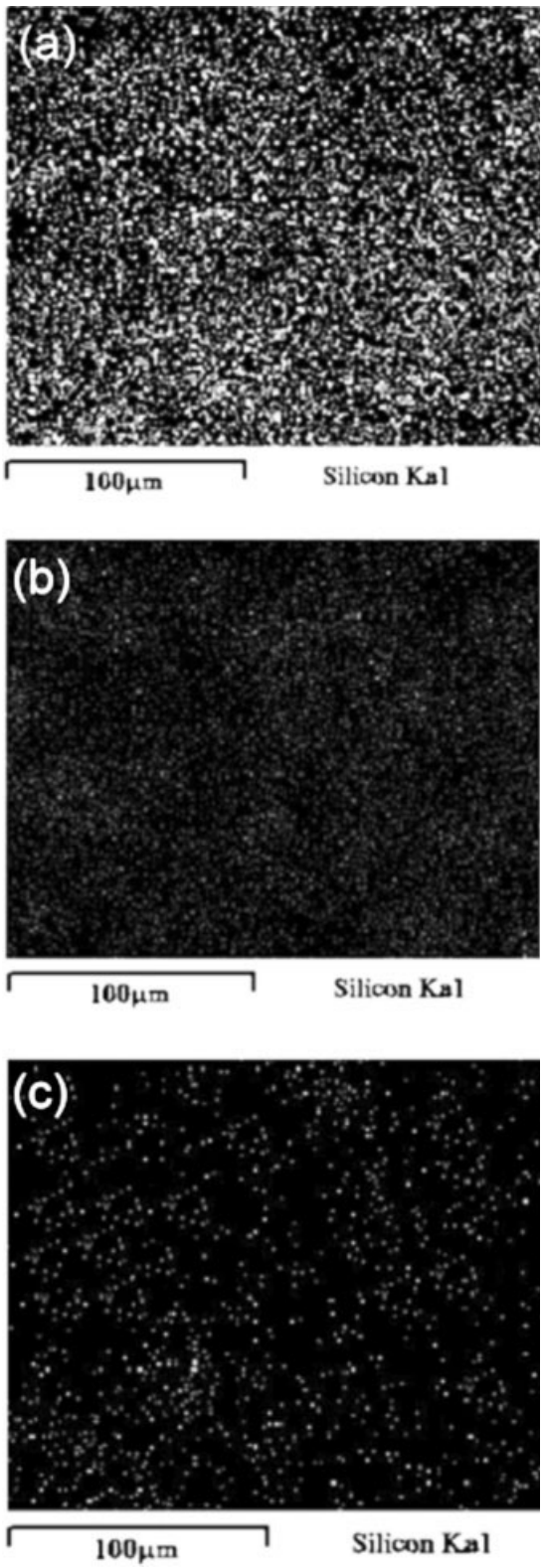

Figure 9 SEM Si mapping micrographs of (a) silica nanoparticles, (b) PS/silica hybrid, and (c) PMMA/silica hybrid.

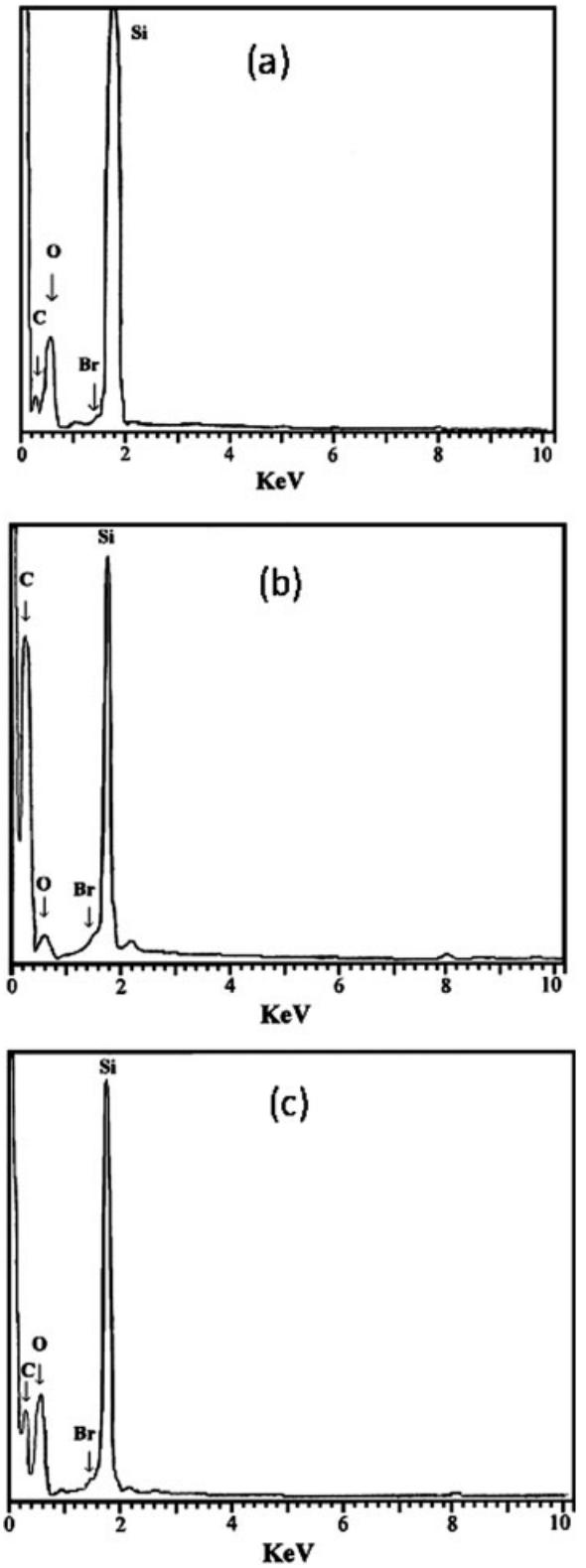

Figure 10 SEM EDS spectra of (a) SiO_2-BIDS initiator, (b) PS/silica hybrid, and (c) PMMA/silica hybrid.

tion, it is apparent that higher O/C ratio was obtained for the PMMA/silica hybrid in comparison with that of PS/silica hybrid. This is reasonable due to more oxygen being present in PMMA polymer.

Thermogravimetric analysis

The thermal stability for neat silica, SiO_2-BIDS initiator and nanohybrids in nitrogen is illustrated in Figure 11. The thermal stabilities of nanohybrids can be enhanced via the formation of organic/inorganic hybrids and uniformly dispersion of silica. As seen in the figure, the TGA curves for silica and SiO_2-BIDS initiator show a continuous degradation mechanism. Before 100°C, a significant weight loss $\sim$ 1.79% is observed for neat silica. It is due to the removal of encapsulated water in nanosilica. Subsequently, a continuous weight loss $\sim$ 5.22% is attributed to the dehydroxylation reaction of surface silanols. Similarly, a weight loss $\sim$ 0.98% is also arising from the water removal for the SiO_2-BIDS initiator. Then, a more rapid weight loss, occurring at $\sim$ 330°C, represents the degradation of BIDS segment, leaving the inorganic part, i.e., silica.

For the PS/silica hybrid, a char residue $\sim$ 51.0% is due to the presence of nanosilica. A lower char residue $\sim$ 42.5% is observed for the PMMA/silica nanohybrid, which is caused by a higher molecular weight (see Table I) of the attached polymer segment.

Contact angle measurements

Contact angle measurements were carried out on glass slides coated with the measured samples to investigate nanoscopic topography of the prepared hybrid materials. The water-repellent and self-cleaning behaviors of micro- and nanostructured plant surfaces are called Lotus effect. It has inspired a significant amount of research on wettability and self-cleaning properties of solid surfaces. Self-cleaning materials usually possess superhydrophilicity or superhydrophobicity.[38] Superhydrophobic surfaces

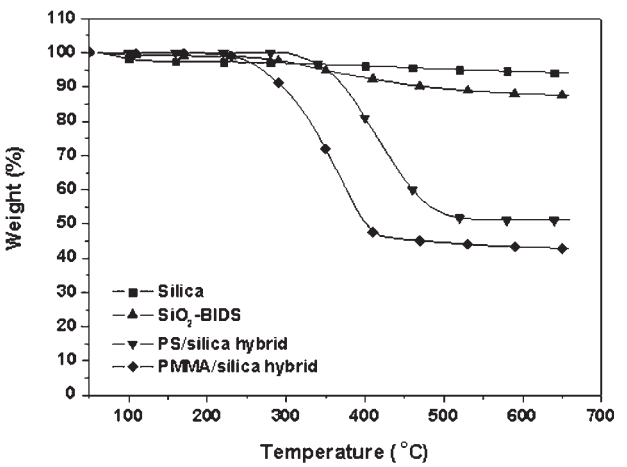

Figure 11 TGA curves of silica nanoparticles, SiO_2-BIDS, PS/silica hybrid, and PMMA/silica hybrid under a nitrogen atmosphere.

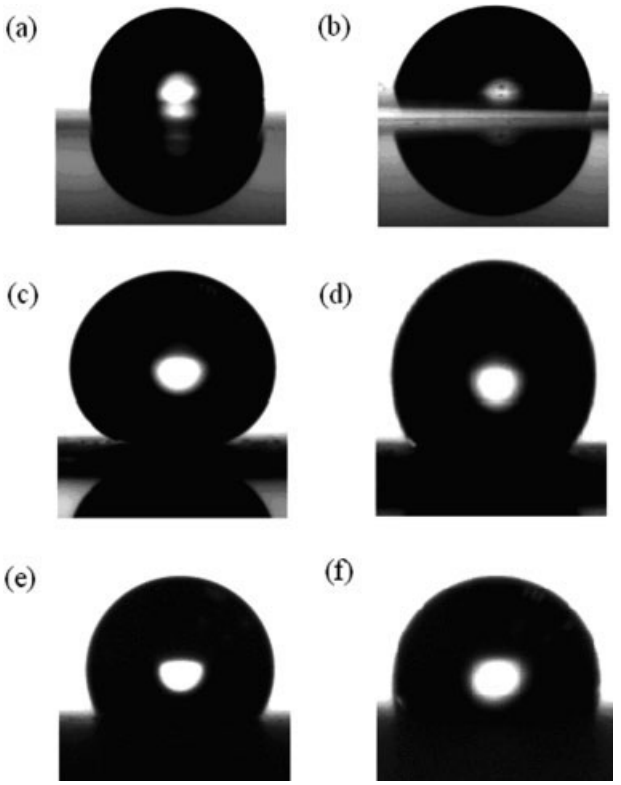

Figure 12 Contact angle photographs of water on the surfaces of glass slides coated with (a) PS (91.5°), (b) PMMA (82.1°), (c) PS/silica hybrid (165.7°), and (d) PMMA/silica hybrid (142.3°), (e) PS/silica blend (116.3°, control), and (f) PMMA/silica blend (105.5°, control).

have usually been produced in two ways: on the basis of geometry and chemistry.[39–41] Our hybrid materials have the characteristic of superhydrophobic surfaces based on the geometry. A main characteristic of superhydrophobic surfaces is a roughness on the micro and nanometer scales. In all experiments a common finding is that the water contact angle increases with surface roughness. Figure 12 shows the effect of different coating materials on the contact angle measurements. For a clean glass slide without any coated materials, the contact angle measured was $\sim 45.0^\circ$.

Figure 12(a,b) show contact angles of water on neat PS and PMMA coated glass slides, respectively. As shown in the figure, the contact angle of water on the PS-coated glass is larger than 90°, indicating PS is normally a hydrophobic material. The contact angle of water on PMMA-coated glass is a little smaller, which reveals that PMMA is more hydrophilic than PS. The reason can be readily explained from the molecular structure of both samples.

On the other hand, contact angle measurements for both nanohybrids exhibit the novel characteristic of nanomaterials. As seen from Figure 12(c), the PS/silica nanohybrid has a contact angle of 165.7°. Even for the more hydrophilic sample of PMMA, a contact angle of 142.3° [Fig. 12(d)] is measured for its hybrid with nanosilica, indicating the molecular structure of PMMA/silica nanohybrid has a distinct structure compared with that of PMMA. It is apparent that both nanohybrids show the characteristic of nanomaterials. Since the PS or PMMA segments were covalently grafted from the silica nanoparticles, the morphology of nanohybrids looked like star-shaped materials carrying radiated polymer segments as shown in Scheme 1. Therefore, an increase in surface roughness was achieved. Consequently, much higher contact angles were obtained due to the very small contact areas of water on the surfaces of polymer/silica nanohybrids. Conversely, if the glass slides were just coated with PS/silica and PMMA/silica blends (used as controls), using the same ratios of organic/inorganic materials similar to the polymer/silica hybrids, it was found that contact angles of water on both glass slides showed only small increases compared to those of neat PS and PMMA coated glass slides [Fig. 12(e,f)]. It is obvious that no much increase on surface roughness for both blend samples. These results testify the nano-character of both organic/inorganic nanohybrids.

CONCLUSIONS

Structurally well-defined PS/silica and PMMA/silica hybrids were prepared by modifying the surfaces of silica nanoparticles with BIDS initiator for ATRP and by using these initiator-modified nanoparticles as macroinitiators. Using ATRP, well-defined polystyrene and poly(methyl methacrylate) chains were grown from the nanoparticle surfaces to yield particles composed of a silica core and a well-defined, densely grafted outer polymer layer. FTIR and solid state ^{13}C and ^{29}Si-NMR spectra were used in the identification of the SiO_2-BIDS initiator and the hybrid materials. The presence of bromine, oxygen, and carbon atoms from SEM EDS spectra also confirmed the successful syntheses of the colloid initiator and both hybrid materials. Both hybrid nanoparticles exhibited higher thermal stabilities and lotus effect (self-cleaning property) compared with neat polymers. The results of SEM and contact angle measurement showed that the organic/inorganic hybrids synthesized by ATRP are nanomaterials.

References

1. Alivisatos, A. P.; Science 1996 (Washington), 271, 933.
2. Moller, M.; Spatz, J. P. Curr Opin Colloid Int Sci 1997, 2, 177.
3. Forster, S.; Antonietti, M. Adv Mater 1998, 10, 195.
4. Golden, J. H.; Deng, H.; DiSalvo, F. J.; Thompson, P. M.; Frechet, J. M. J Science (Washington) 1995, 268, 1463.
5. Wen, J.; Wilkes, G. L. Chem Mater 1996, 8, 1667.

6. Mori, H.; Seng, D. C.; Zhang, M.; Muller, A. H. E. Langmuir 2002, 18, 3682.
7. Suzuki, K.; Siddiqui, S.; Chappell, C.; Siddiqui, J. A.; Ottenbrite, R. M. Polym Adv Technol 2000, 11, 92.
8. Caruso, F.; Móhwald, H. Langmuir 1999, 15, 8276.
9. Bourgeat-Lami, E.; Lang, J. J Colloid Interface Sci 1998, 197, 293.
10. Jethmalani, J. M.; Ford, W. T. Chem Mater 1996, 8, 2138.
11. Liu, P.; Tian, J.; Liu, W. M.; Xue, Q. J Chem Bull 2003, 67, 73.
12. Pyun, J.; Matyjaszewski, K. Chem Mater 2001, 13, 3436.
13. Matyjaszewski, K.; Xia, J. H. Chem Rev 2001, 101, 2921.
14. Böttcher, H.; Hallensleben, M. L.; Nu, S.; Wurm, H. Polym Bull 2000, 44, 223.
15. Shirai, Y.; Shirai, K.; Tsubokawa, N. J Polym Sci Part A: Polym Chem 2001, 39, 2157.
16. Carrot, G.; Diamanti, S.; Manuszak, M.; Charleux, B.; Vairon, J. P. J Polym Sci Part A: Polym Chem 2001, 39, 4294.
17. Von Werne, T.; Patten, T. E. J Am Chem Soc 2001, 123, 7497.
18. Von Werne, T.; Patten, T. E. J Am Chem Soc 1999, 121, 7409.
19. Farmer, S. C.; Patten, T. E. Chem Mater 2001, 13, 3920.
20. Savin, D. A.; Pyun. J.; Patterson, G. D.; Kowalewski, T.; Matyjaszewski, K. J Polym Sci Part B: Polym Phys 2002, 40, 2667.
21. Chen, X.; Randall, D. P.; Perruchot, C.; Watts, J. F.; Patten, T. E.; Von Werne, T.; Armes, S. P. J Colloid Interface Sci 2003, 257, 56.
22. Nuss, S.; Bottcher, H.; Wurm, H.; Hallensleben, M. L. Angew Chem Int Ed Engl 2001, 40, 4016.
23. Mandal, T. K.; Fleming, M. S.; Walt, D. R. Nano Lett 2002, 2, 3.
24. Ohno, K.; Koh, K. M.; Tsujii, Y.; Fukuda, T. Macromolecules 2002, 35, 8989.
25. Zhu, M. Q.; Wei, L. H.; Zhang, W. C.; Du, F. S.; Li, Z. C., Li, F. M. Polym Prepr (Am Chem Soc Div Polym Chem) 2002, 43, 68.
26. Tanke, R. S.; Kauzlarich, S. M.; Patten, T. E.; Pettigrew, K. A.; Murphy, D. L.; Thompson, M. E.; Lee, H. W. H. Chem Mater 2003, 15, 1682.
27. Tsubokawa, N.; Yoshikawa, S. Rec Res Dev Polym Sci 1998, 2, 211.
28. Wang, J. Y.; Chen, W.; Liu, A. H.; Lu, G.; Zhang, G.; Zhang, J. H.; Yang, B. J Am Chem Soc 2002, 124, 13358.
29. Kickelbick, G.; Holzinger, D.; Brick, C.; Trimmel, G.; Moons, E. Chem Mater 2002, 14, 4382.
30. Gu, B.; Sen, A. Macromolecules 2002, 35, 8913.
31. Costa, R. O. R.; Vasconcelos, W. L.; Tamaki, R.; Laine, R. M.; Macromolecules 2001, 34, 5398.
32. Zhao, B.; Brittian, W. J Prog Polym Sci 2000, 25, 677.
33. Qiu, J.; Charleux, B.; Matyjaszewski, K. Prog Polym Sci 2001, 26, 2083.
34. Pyun, J.; Jia, S.; Kowalewski, T.; Patterson, G. D. Matyjaszwski, K. Macromolecules 2003, 36, 5094.
35. Ding, S.; Yung, J.; Radosz, M.; Shen, Y. J Polym Sci Part A: Polym Chem 2004, 42, 22.
36. Costa, R. O. R.; Vasconcelos, W. L.; Tamaki, R.; Laine, R. M. Macromolecules 2001, 34, 16.
37. Liu, P.; Tain, J.; Liu, W; Xue, Q. Polym Int 2004, 53, 127.
38. Geo, Y.; Masuda, Y.; Koumoto, K. Langmuir 2004, 20, 3188.
39. Achim, W. H.; Srdjan, M.; Ulrich, S.; Henry, G.; Vladimir, Z.; Rainer, A.; Franz, F. Langmuir 2091 2007, 23.
40. Wenzel, R. N. Ind Eng Chem 1936, 28, 988.
41. Cassie, A. B. D.; Baxter, S. Trans Faraday Soc 1944, 40, 546.